0090-9556/06/3411-1793–1797$20.00
DRUG METABOLISM AND DISPOSITION
Vol. 34, No. 11
10488/3145364
DMD 34:1793–1797, 2006
Printed in U.S.A.
Copyright © 2006 by The American Society for Pharmacology and Experimental Therapeutics

Short Communication

Characterization of Ebastine, Hydroxyebastine, and Carebastine Metabolism by Human Liver Microsomes and Expressed Cytochrome P450 Enzymes: Major Roles for CYP2J2 and CYP3A

Received April 9, 2006; accepted August 1, 2006

ABSTRACT:

Ebastine undergoes extensive metabolism to form desalkylebastine and hydroxyebastine. Hydroxyebastine is subsequently metabolized to carebastine. Although CYP3A4 and CYP2J2 have been implicated in ebastine *N*-dealkylation and hydroxylation, the enzyme catalyzing the subsequent metabolic steps (conversion of hydroxyebastine to desalkylebastine and carebastine) have not been identified. Therefore, we used human liver microsomes (HLMs) and expressed cytochromes P450 (P450s) to characterize the metabolism of ebastine and that of its metabolites, hydroxyebastine and carebastine. In HLMs, ebastine was metabolized to desalkyl-, hydroxy-, and carebastine; hydroxyebastine to desalkyl- and carebastine; and carebastine to desalkylebastine. Of the 11 cDNA-expressed P450s, CYP3A4 was the main enzyme catalyzing the *N*-dealkylation of ebastine, hydroxyebastine, and carebastine to desalkylebastine [intrinsic clearance (CL_{int}) = 0.44, 1.05, and 0.16 μl/min/pmol P450, respectively]. Ebastine and hydroxyebastine were also dealkylated to desalkylebastine to some extent by CYP3A5. Ebastine hydroxylation to hydroxyebastine is mainly mediated by CYP2J2 (0.45 μl/min/pmol P450; 22.5- and 7.5-fold higher than that for CYP3A4 and CYP3A5, respectively), whereas CYP2J2 and CYP3A4 contributed to the formation of carebastine from hydroxyebastine. These findings were supported by chemical inhibition and kinetic analysis studies in human liver microsomes. The CL_{int} of hydroxyebastine was much higher than that of ebastine and carebastine, and carebastine was metabolically more stable than ebastine and hydroxyebastine. In conclusion, our data for the first time, to our knowledge, suggest that both CYP2J2 and CYP3A play important roles in ebastine sequential metabolism: dealkylation of ebastine and its metabolites is mainly catalyzed by CYP3A4, whereas the hydroxylation reactions are preferentially catalyzed by CYP2J2. The present data will be very useful to understand the pharmacokinetics and drug interaction of ebastine in vivo.

Ebastine, a potent and selective histamine H_1-receptor antagonist, belongs to a second generation of nonsedating antihistamines but with negligible anticholinergic and antiserotonergic properties (Llupia et al., 2003). Ebastine undergoes extensively sequential metabolism in the liver (Hashizume et al., 1998, 2001). The major primary metabolites identified in humans are hydroxy- and desalkylebastine, and hydroxyebastine is further metabolized to carebastine. In vitro studies indicate that the formation of desalkyl- and hydroxyebastine from ebastine is catalyzed by CYP3A4 and CYP2J2, respectively (Hashizume et al., 2002). The specific hepatic cytochrome P450 (P450) enzymes involved in hydroxy- and carebastine metabolism have not been identified so far, despite some information which could be obtained from the previously published pharmacokinetics of ebastine. After oral administration to experimental animals and humans, ebastine is almost completely metabolized to the pharmacologically active principle, the carboxylated metabolite (carebastine), and other inactive metabolites (desalkylebastine) (Yamaguchi et al., 1994; Rohatagi et al., 2001). The C_{max} value of hydroxyebastine, the major metabolite of ebastine in vitro, was approximately 50-fold lower than that of carebastine in vivo (Kang et al., 2004). A recent study by Chaikin et al. (2005) has reported that ketoconazole, a potent inhibitor of CYP3A4-mediated metabolism, decreases the clearance of ebastine, leading to an accumulation of the ebastine, with little effect on the pharmacokinetics of carebastine. However, since they did not measure the change of the intermediate metabolite, hydroxyebastine, it is still open to question which P450 isoforms may contribute to the formation of carebastine.

The objective of this study was to identify and kinetically characterize in vitro the P450 isoforms responsible for the metabolism of ebastine and its metabolites. The information from these studies will allow better understanding of the factors affecting ebastine pharmacokinetics and drug interaction.

This work was supported by a grant from the Ministry of Science and Technology, Korea (National Research Laboratory Program) and the Korea Health 21 R & D Project, Ministry of Health & Welfare, R. O. K (03-PJ10-PG13-GD01-0002).

Article, publication date, and citation information can be found at http://dmd.aspetjournals.org.

doi:10.1124/dmd.106.010488.

Materials and Methods

Chemicals and Reagents. Ebastine, desalkylebastine, hydroxyebastine, and carebastine were kindly donated by Almirall Prodesfarma, SA (Barcelona, Spain). Astemizole, coumarin, diethyldithiocarbamate, furafylline, ketoconazole, quinidine, sulfaphenazole, terfenadine, thio-TEPA, β-nicotinamide adenine dinucleotide phosphate, EDTA, $MgCl_2$, glucose 6-phosphate, and glu-

ABBREVIATIONS: P450, cytochrome P450; HLM, human liver microsome; thio-TEPA, triethylenethiophosphoramide; LC/MS/MS, liquid chromatography-tandem mass spectrometry; CL_{int}, intrinsic clearance.

cose-6-phosphate dehydrogenase were purchased from Sigma-Aldrich (St. Louis, MO). Solvents were high-performance liquid chromatography-grade (Fisher Scientific Co., Pittsburgh, PA) and the other chemicals were of the highest quality available. Pooled (H161) or single-donor (H003, H056, and HK34) human liver microsomes (HLMs), and 11 different human recombinant P450 isoforms, 1A2, 2A6, 2B6, 2C8, 2C9, 2C19, 2D6, 2E1, 2J2, 3A4, and 3A5 (Supersomes), were purchased from BD Gentest (Woburn, MA). Human P450s 2A6, 2B6, 2C8, 2C9, 2C19, 2E1, 2J2, 3A4, and 3A5 are coexpressed with human P450 reductase and cytochrome b_5; however, P450s 1A2 and 2D6 are only coexpressed with human P450 reductase. The manufacturer supplied information regarding protein concentration and P450 isoform content.

Metabolism of Ebastine and Its Metabolites in Human Liver Microsomes or Expressed P450s. The optimal conditions for microsomal incubation were determined in the linear range for the formation of metabolites of ebastine, hydroxyebastine, and carebastine. The rates of formation of metabolites were proportional to incubation times up to 60 min and protein concentrations up to 1.0 mg/ml at 30 min. In all experiments, ebastine, hydroxyebastine, and carebastine were dissolved and serially diluted with methanol to the required concentrations; the solvent was subsequently removed by evaporation to dryness, under reduced pressure with an AES2010 SpeedVac (Thermo Electron Corporation, Waltham, MA).

The incubation mixtures, containing either 25 μl of microsomes (2.5 mg of protein/ml of stock, prepared from three different human liver microsomal preparations) or 25 μl of cDNA-expressed P450 (diluted to 200 pmol/ml with phosphate buffer, pH 7.4) and various concentrations of ebastine, hydroxyebastine, or carebastine (0–100 μM) was reconstituted in 100 μM phosphate buffer (pH 7.4) and prewarmed for 5 min at 37°C. The reaction was initiated by adding the NADPH-regenerating system (1.3 mM β-nicotinamide adenine dinucleotide phosphate, 3.3 mM glucose 6-phosphate, 3.3 mM $MgCl_2$, and 1.0 U/ml glucose-6-phosphate dehydrogenase) and further incubated (final volume of 250 μl) for 30 min at 37°C in a shaking water bath. The reaction was terminated by placing the incubation tubes on ice and by immediately adding 100 μl of acetonitrile. After adding the internal standard (terfenadine, 1 μM), the mixture was centrifuged at 1000*g* for 5 min at 4°C and aliquots of the supernatant were injected into an LC/MS/MS system.

Chemical Inhibition Studies with Human Liver Microsomes. Pooled HLMs (H161, pooled from 27 individual microsomes) and a P450-selective inhibitor were added to an incubation mixture similar to that described above. Ebastine, hydroxyebastine, and carebastine concentrations were 5 μM. The P450 isoform-selective inhibitors used were furafylline (10 μM) for CYP1A2, coumarin for CYP2A6 (100 μM), thio-TEPA for CYP2B6 (5 μM), sulfaphenazole for CYP2C9 (10 μM), *S*-benzylnirvanol for CYP2C19 (1 μM), quinidine for CYP2D6 (10 μM), diethyldithiocarbamate for CYP2E1 (10 μM), and ketoconazole for CYP3A (1 μM). Astemizole (50 μM), a substrate of CYP2J2 and CYP3A4, was used as competitive inhibitor. Except for the addition of P450 isoform-selective inhibitors, all other incubation conditions were similar to those described previously by our group (Shin et al., 1999, 2002). After adding the internal standard and centrifugation as described above, aliquots of the supernatant were analyzed on an LC/MS/MS system.

Analytical Procedures. The concentrations of desalkyl-, hydroxy-, and carebastine were measured by LC/MS/MS as described elsewhere (Kang et al., 2004). The system consisted of an API 3000 LC/MS/MS system (Applied Biosystems, Foster City, CA) equipped with an electrospray ionization interface used to generate positive ions $[M + H]^+$. The compounds were separated on a reversed-phase column (Luna C_{18}, 2.0 mm i.d. $\times$ 50 mm, 3-μm particle size; Phenomenex, Torrance, CA) with an isocratic mobile phase consisting of acetonitrile and water (40/60 v/v) containing 0.1% formic acid. The mobile phase was eluted using an HP 1100 series pump (Agilent, Wilmington, DE) at 0.2 ml/min.

The Turboion Spray interface was operated in the positive ion mode at 5500 V and 375°C. The operating conditions were determined as follows: nebulizing gas flow, 1.04 l/min; auxiliary gas flow, 4.0 l/min; curtain gas flow, 1.44 l/min; orifice voltage, 40 V; ring voltage, 350 V; collision gas (nitrogen) pressure, 3.58×10^{-5} Torr. The mass transitions used for quantitation of hydroxyebastine, carebastine, and terfenadine were *m/z* 486.7 $\rightarrow$ 167.1, 500.6 $\rightarrow$ 167.1, and 472.7 $\rightarrow$ 436.0, respectively (collision energy 40 eV): that for desalkylebastine was *m/z* 268.4 $\rightarrow$ 167.1 (collision energy 15 eV). The analytical data were processed by Analyst software (version 1.2; Applied Biosystems).

Data Analysis. Results are expressed as means $\pm$ S.D. of estimates obtained from three different liver microsome preparations in duplicate experiments. The apparent kinetic parameters of ebastine, hydroxyebastine, and carebastine metabolism were determined by fitting the unweighted kinetic data from HLMs and expressed P450s to a one-enzyme Michaelis-Menten equation or a sigmoidal (Hill) equation model [$V = V_{max} \cdot [S]^n/(K_m^n + [S]^n)$], or a substrate inhibition model [$V = V_{max}/(1 + K_m/[S] + [S]/K_{si})$]. Calculated parameters were maximum rate of metabolite formation (V_{max}), Michaelis constant (K_m), intrinsic clearance ($CL_{int} = V_{max}/K_m$), Hill coefficient (n), and substrate inhibition constant (K_{si}). The percentages of inhibition were calculated by the ratio of the rate of metabolite formation with and without the specific inhibitor. Calculations were performed using WinNonlin software (Pharsight, Mountain View, CA).

Results and Discussion

We present here a detailed characterization of the in vitro metabolism of ebastine and its metabolites using human liver P450 enzymes as summarized in Fig. 1. We have demonstrated that: 1) ebastine undergoes primary oxidative hydroxylation of the methyl groups of the *tert*-butyl moiety of ebastine to hydroxyebastine and dealkylation at the alicyclic bond attached to the piperidine nitrogen to form desalkylebastine, and secondary metabolism to carebastine; 2) the major route(s) of ebastine metabolism is mainly catalyzed by CYP2J2, CYP3A4, and CYP3A5; and 3) CYP2J2 exhibits atypical kinetics. These data should provide a scientific base upon which to build focused clinical studies that will help in understanding the pharmacokinetics and pharmacogenetic factors influencing ebastine therapeutic efficacy, drug interactions, and safety.

The formation of metabolites followed simple Michaelis-Menten kinetics with 0~100 μM ebastine, hydroxyebastine, or carebastine, suggesting the involvement of a single enzyme or more than one enzyme with similar affinity (Fig. 2). A similar kinetic profile has been observed with ebastine hydroxylation in human intestinal microsomes (Hashizume et al., 2002) and CYP2J2-mediated terfenadine hydroxylation in recombinant CYP2J2 (Parikh et al., 2003). The kinetic parameters are summarized in Table 1. The formation of carebastine from hydroxyebastine by rCYP2J2 exhibited substrate inhibition (Fig. 3), unlike the kinetic data obtained in HLMs, which were characterized by a hyperbolic Michaelis-Menten equation (Fig. 2). Comparison of the goodness-of-fit values generated from these data indicates that a substrate inhibition enzyme kinetic model provided a better fit than did other models. The corresponding Eadie-Hofstee plot indicated a "hook" in the upper region of this plot (Fig. 3B, inset), which is characteristic of substrate inhibition. The K_m,

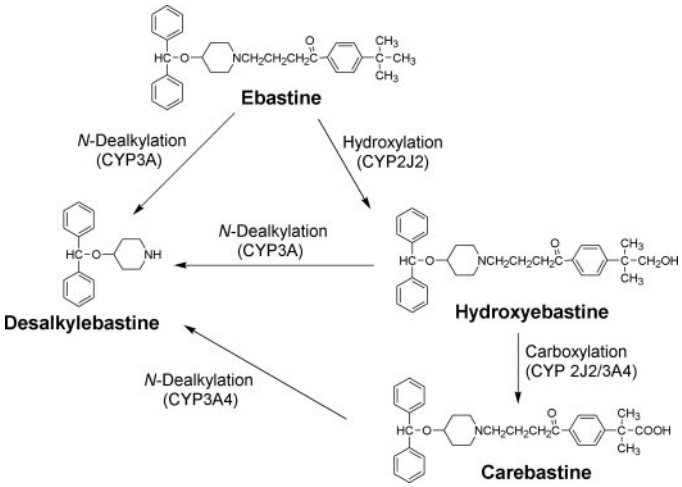


FIG. 1. Proposed metabolic pathway of ebastine in human liver microsomes.

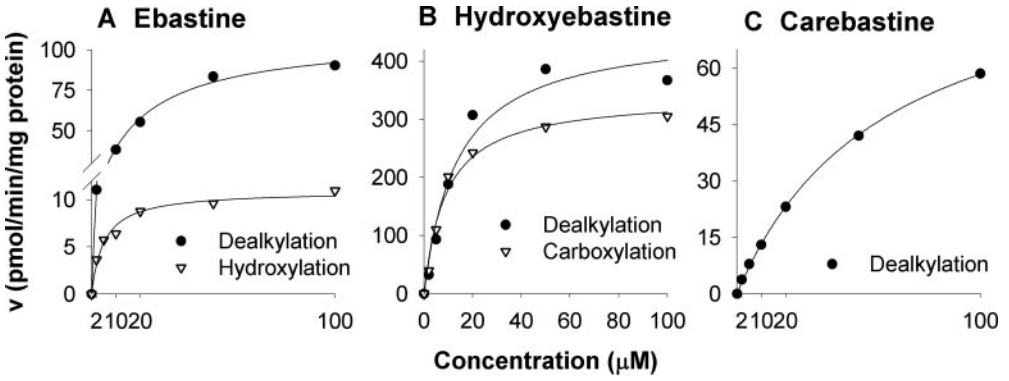


FIG. 2. Kinetics for the metabolite formation from ebastine (A), hydroxyebastine (B), and carebastine (C) in three human liver microsomes. An increasing concentration of substrates (0–100 μM) was incubated with human liver microsomes and an NADPH-generating system at 37°C for 30 min. The velocity (pmol/min/mg protein) versus substrate concentration was fit to a Michaelis-Menten equation (see "*Data Analysis*" under *Materials and Methods*). Each point represents the average obtained from three different human liver microsomes.

TABLE 1

Kinetic parameters for the metabolism of ebastine, hydroxyebastine, and carebastine in human liver microsomes

The values are estimated from nonlinear least regression analysis using WinNonlin.

Kinetic Parameters	V_{max}	K_m	V_{max}/K_m
	pmol/min/mg protein	*μM*	*μl/min/mg protein*
Ebastine			
Dealkylation	108.2 ± 29.6	17.5 ± 2.3	6.18 ± 1.16
Hydroxylation	10.9 ± 3.0	5.1 ± 1.3	2.14 ± 0.48
Hydroxyebastine			
Dealkylation	456.4 ± 69.1	13.7 ± 3.8	33.3 ± 9.0
Carboxylation			
Carebastine	340.2 ± 64.1	8.9 ± 0.9	38.2 ± 6.5
Dealkylation	94.1 ± 27.0	61 ± 6.1	1.54 ± 0.51

V_{max}, and K_{si} estimated from these data, respectively, were 0.75 μM, 9.86 pmol/min/pmol P450, and 5.55 μM (Table 2). Similar substrate inhibition profiles have been observed previously with CYP2B6-mediated 8,14-dihydroxyefavirenz formation (Ward et al., 2003) and CYP3A-mediated triazolam hydroxylation (Schrag and Wienkers, 2001), which are suggestive of multiple substrate-binding sites (or multiple regions within a single active site). To our knowledge, this is the first report of CYP2J2-mediated substrate inhibition. Although this observation may have no clinical relevance because the expected concentrations of the hydroxyebastine in human plasma after taking the usual dosage of ebastine (Kang et al., 2004) are much lower than the substrate inhibition constants we obtained here, it may offer insight into the characteristics of the enzyme.

We provide evidence that ebastine hydroxylation is predominantly catalyzed by CYP2J2. First, formation rates of hydroxyebastine were potently inhibited (~70%) by astemizole, a substrate of CYP2J2 and CYP3A4, and slightly inhibited by ketoconazole, a potent CYP3A-selective inhibitor (Fig. 4A). Second, expressed human CYP2J2 metabolized ebastine to hydroxyebastine, whereas other P450 isoforms did not (Fig. 5A). We also noted that recombinant human CYP3A4 formed hydroxyebastine from ebastine, but the contributions of this isoform to ebastine metabolism appear minor: 1) the CL_{int} for hydroxyebastine formation by CYP3A4 was 22.5-fold lower than that obtained in recombinant human CYP2J2 (Table 2); and 2) a CYP3A-specific inhibitor (ketoconazole) slightly inhibited (~25%) the rates of formation of hydroxyebastine in HLMs (Fig. 4A). These qualitative findings are consistent with the earlier work which had reported that CYP2J2 is the predominant ebastine hydroxylase in human intestinal microsomes (Hashizume et al., 2002).

The specific hepatic P450 enzymes involved in hydroxy- and carebastine metabolism have not been identified so far. Both ketoconazole (CYP3A inhibitor) and astemizole (substrate of CYP2J2 and CYP3A4) (Matsumoto et al., 2003) markedly inhibited (>82%) car- and desalkylebastine formation (Fig. 4, B and C). Human recombinant CYP2J2 and CYP3A4 formed carebastine from hydroxyebastine (Fig. 5B). Similar to desalkylebastine formation from ebastine, desalkylebastine formation from hydroxy- and carebastine was mediated by CYP3A enzyme only (Fig. 5). These results suggest that desalkylebastine formation from hydroxy- and carebastine was clearly mediated by CYP3A, and hydroxyebastine was oxidized to carebastine by CYP2J2 and CYP3A4. It would be interesting to consider the enzymes responsible for metabolism of terfenadine alcohol, which possesses chemical structural similarities to hydroxyebastine. Terfenadine alcohol also has two similar major metabolic pathways of carboxylation and *N*-dealkylation. Unlike hydroxyebastine, carboxylation of terfenadine alcohol is reported to be catalyzed predominantly

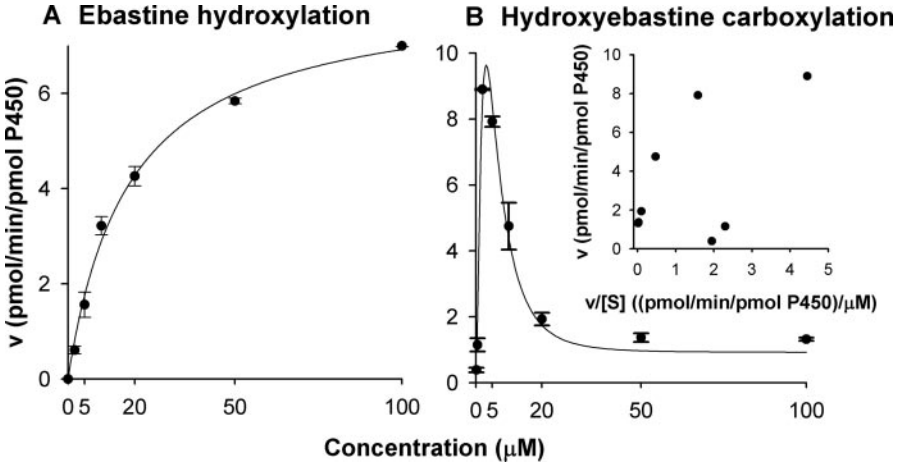


FIG. 3. Kinetics for the metabolite formation from ebastine (A) and hydroxyebastine (B) in recombinant human CYP2J2. An increasing concentration of substrates (0–100 μM) was incubated with recombinant human CYP2J2 and an NADPH-generating system at 37°C for 30 min. The velocity (pmol/min/pmol P450) versus ebastine or hydroxyebastine concentration was fit to a Michaelis-Menten equation or substrate inhibition equation (see "*Data Analysis*" under *Materials and Methods*). The corresponding Eadie-Hofstee plot (velocity versus velocity/hydroxyebastine concentration) is shown in the inset. Each point represents the average ± S.D. of triplicate incubations.

TABLE 2

Kinetic parameters for the metabolism of ebastine, hydroxyebastine, and carebastine in recombinant human P450s

The values are estimated from nonlinear least regression analysis using WinNonlin.

Kinetic Parameters		V_{max}	K_m	V_{max}/K_m
		pmol/min/pmol P450	*μM*	*μl/min/pmol P450*
CYP3A4	Ebastine			
	Dealkylation	3.34	7.67	0.44
	Hydroxylation	0.12	6.86	0.02
	Hydroxyebastine			
	Dealkylation	7.99	7.63	1.05
	Carboxylation	1.10	3.48	0.32
	Carebastine			
	Dealkylation	0.60	3.85	0.16
CYP3A5	Ebastine	0.74	5.56	0.13
	Dealkylation			
	Hydroxylation	0.14	2.33	0.06
	Hydroxyebastine			
	Dealkylation	3.09	21.9	0.14
	Carboxylation	0.79	13.6	0.06
CYP2J2	Ebastine			
	Hydroxylation	8.20	18.3	0.45
	Hydroxyebastine			
	Carboxylation	9.86	0.75	

by CYP3A4 (Ling et al., 1995). However, the previous study did not evaluate CYP2J2-mediated metabolism. Based on recent results (Parikh et al., 2003), which reported that CYP2J2 is a major enzyme involved in terfenadine (structural analog of ebastine) hydroxylation, we can speculate that CYP2J2 as well as CYP3A4 may be involved in terfenadine acid formation from terfenadine alcohol.

After oral administration to humans, ebastine is almost completely metabolized to car- and desalkylebastine (Kang et al., 2004; Lasseter et al., 2004). It is inconsistent with the in vitro findings, which reported that ebastine is predominantly metabolized to hydroxy- and desalkylebastine (Hashizume et al., 1998, 2001, 2002). To clarify this, we performed an in vitro metabolism study of ebastine as well as its metabolites, hydroxy- and carebastine, using human liver microsomes. The intrinsic clearance of hydroxyebastine was much higher than that of ebastine and carebastine (Table 1). The ratio of maximum dealkylation rate (V_{max}) of hydroxyebastine was also higher than that of ebastine and carebastine. In contrast to hydroxyebastine, carebastine showed low enzyme affinity and metabolic rate, thus resulting in relatively low metabolic clearance. In expressed P450s, the formation of hydroxy- and desalkylebastine from ebastine was catalyzed predominantly by CYP2J2 and CYP3A4, respectively (Table 2). When hydroxyebastine was used as a substrate, we concluded that CYP2J2 and CYP3A4 isoforms were responsible for oxidation of hydroxyebastine, whereas CYP3A4 and CYP3A5 were responsible for desalkylebastine formation. Kinetic analysis indicated that the intrinsic clearance of hydroxyebastine was much higher than that of ebastine and carebastine (Table 1). These results provide evidence that once the hydroxyebastine is formed, it undergoes a rapid biotransformation to yield car- and desalkylebastine. Carebastine seems to be relatively metabolically stable to ebastine and hydroxyebastine, supporting the in vivo findings that carebastine is a major metabolite of ebastine. In addition, it is important to note, however, that CYP2J2 is also expressed in the extrahepatic tissues such as heart, intestine, and kidney. Therefore, in vitro metabolism study using extrahepatic tissues such as intestinal microsomes is necessary to determine the contribution of extrahepatic tissues in the metabolism of ebastine and its metabolites.

The identification of CYP2J2 as the catalyst of hydroxylation of ebastine and hydroxyebastine (Fig. 1) may allow us to use ebastine to probe this enzyme system. Despite the identification of a growing list of clinically important drugs (Hashizume et al., 2001; Matsumoto et al., 2003; Parikh et al., 2003) and endogenous substances (Wu et al., 1996; Hashizume et al., 2002) as substrates of CYP2J2 in vitro, it remains difficult to determine or predict its clinical consequences because of the unavailability of a specific and safe probe to measure

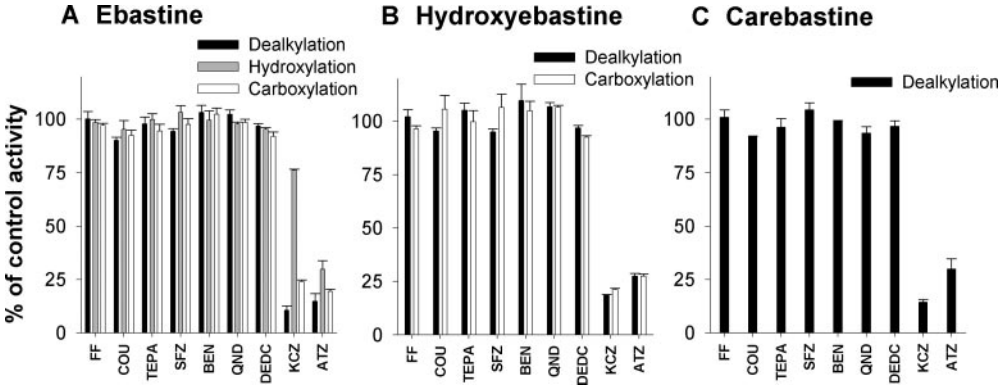


FIG. 4. Effects of P450 isoform-selective inhibitors on the metabolism of ebastine (A), hydroxyebastine (B), and carebastine (C) by human liver microsomes. Ebastine, hydroxyebastine, or carebastine (5 μM) was incubated with pooled human liver microsomes in the presence of various inhibitors. Data are presented as mean ± S.D. of triplicate determinations. FF, furafylline (10 μM); COU, coumarin (100 μM); TEPA, thio-TEPA (5 μM); SFZ, sulfaphenazole (10 μM); BEN, *S*-benzylnirvanol (1 μM); QND, quinidine (10 μM); DEDC, diethyldithiocarbamate (10 μM); KCZ, ketoconazole (1 μM); ATZ, astemizole (50 μM).

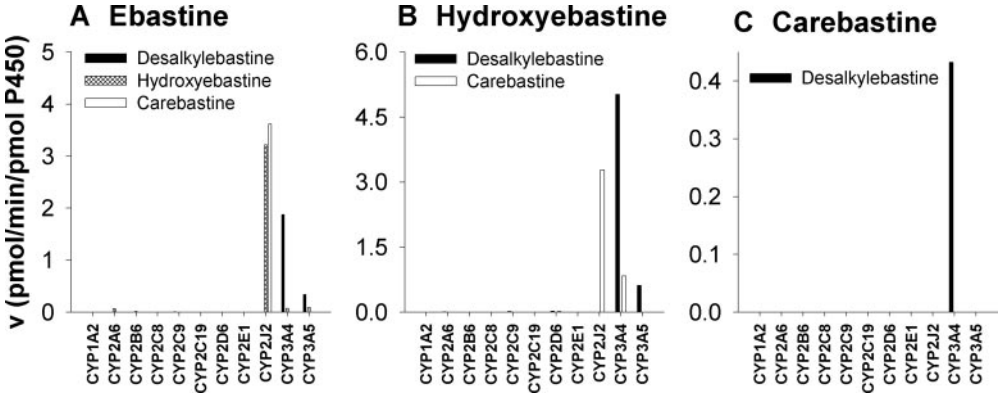


FIG. 5. Representative plots of the formation of each metabolite from ebastine (A), hydroxyebastine (B), and carebastine (C) by cDNA-expressed human P450 isoforms. Human cDNA-expressed P450s 1A2, 2A6, 2B6, 2C8, 2C9, 2C19, 2D6, 2E1, 2J2, 3A4, and 3A5 were incubated with 5 μM ebastine, hydroxyebastine, or carebastine. Data shown are averages of triplicate experiments.

the activity of the enzyme in vivo. Our data indicate that ebastine hydroxylation is a specific in vitro reaction marker of CYP2J2 and may have utility as a phenotyping tool to study the role of this enzyme in human drug metabolism.

Department of Pharmacology and PharmacoGenomics Research Center, Inje University College of Medicine, Busan, Korea (K.-H.L., M.-G.K., D.-J.L., Y.-J.Y., M.-J.K., J.-H.S., J.-G.S.); Kwang-Hyeon Liu, Mi-Gyung Kim, Dong-Jun Lee, Yune-Jung Yoon, Min-Jung Kim, Ji-Hong Shon

Department of Surgery, Busan Paik Hospital, Busan, Korea (C.S.C., Y.K.C.); Chang Soo Choi, Young Kil Choi

Frontier Inje Research for Science and Technology, Inje University, Busan, Korea (K.-H.L.); and Division of Clinical Pharmacology, Departments of Medicine and Pharmacology, Indiana University School of Medicine, Indianapolis, Indiana (Z.D.) Zeuresenay Desta, Jae-Gook Shin

References

Chaikin P, Gillen MS, Malik M, Pentikis H, Rhodes GR, and Roberts DJ (2005) Co-administration of ketoconazole with H1-antagonists ebastine and loratadine in healthy subjects: pharmacokinetic and pharmacodynamic effects. *Br J Clin Pharmacol* **59:**346–354.

Hashizume T, Imaoka S, Mise M, Terauchi Y, Fujii T, Miyazaki H, Kamataki T, and Funae Y (2002) Involvement of CYP2J2 and CYP4F12 in the metabolism of ebastine in human intestinal microsomes. *J Pharmacol Exp Ther* **300:**298–304.

Hashizume T, Mise M, Matsumoto S, Terauchi Y, Fujii T, Imaoka S, Funae Y, Kamataki T, and Miyazaki H (2001) A novel cytochrome P450 enzyme responsible for the metabolism of ebastine in monkey small intestine. *Drug Metab Dispos* **29:**798–805.

Hashizume T, Mise M, Terauchi Y, O L, Fujii T, Miyazaki H, and Inaba T (1998) N-Dealkylation and hydroxylation of ebastine by human liver cytochrome P450. *Drug Metab Dispos* **26:**566–571.

Kang W, Liu KH, Ryu JY, and Shin JG (2004) Simultaneous determination of ebastine and its three metabolites in plasma using liquid chromatography-tandem mass spectrometry. *J Chromatogr B Analyt Technol Biomed Life Sci* **813:**75–80.

Lasseter KC, Dilzer SC, Vargas R, Waldman S, and Noveck RJ (2004) Pharmacokinetics and safety of ebastine in patients with impaired hepatic function compared with healthy volunteers: a phase I open-label study. *Clin Pharmacokinet* **43:**121–129.

Ling KH, Leeson GA, Burmaster SD, Hook RH, Reith MK, and Cheng LK (1995) Metabolism of terfenadine associated with CYP3A(4) activity in human hepatic microsomes. *Drug Metab Dispos* **23:**631–636.

Llupia J, Gras J, and Llenas J (2003) Comparative antiallergic effects of second-generation H1-antihistamines ebastine, cetirizine and loratadine in preclinical models. *Arzneim-Forsch* **53:**93–97.

Matsumoto S, Hirama T, Kim HJ, Nagata K, and Yamazoe Y (2003) In vitro inhibition of human small intestinal and liver microsomal astemizole O-demethylation: different contribution of CYP2J2 in the small intestine and liver. *Xenobiotica* **33:**615–623.

Parikh S, Gagne P, Miller V, Crespi C, Thummel K, and Patten C (2003) CYP2J2 and CYP4F12 are active for the metabolism of non-sedating antihistamines: terfenadine and astemizole. *Drug Metab Rev* **35:**190.

Rohatagi S, Gillen M, Aubeneau M, Jan C, Pandit B, Jensen BK, and Rhodes G (2001) Effect of age and gender on the pharmacokinetics of ebastine after single and repeated dosing in healthy subjects. *Int J Clin Pharmacol Ther* **39:**126–134.

Schrag ML and Wienkers LC (2001) Triazolam substrate inhibition: evidence of competition for heme-bound reactive oxygen within the CYP3A4 active site. *Adv Exp Med Biol* **500:**347–350.

Shin JG, Park JY, Kim MJ, Shon JH, Yoon YR, Cha IJ, Lee SS, Oh SW, Kim SW, and Flockhart DA (2002) Inhibitory effects of tricyclic antidepressants (TCAs) on human cytochrome P450 enzymes in vitro: mechanism of drug interaction between TCAs and phenytoin. *Drug Metab Dispos* **30:**1102–1107.

Shin JG, Soukhova N, and Flockhart DA (1999) Effect of antipsychotic drugs on human liver cytochrome P-450 (CYP) isoforms in vitro: preferential inhibition of CYP2D6. *Drug Metab Dispos* **27:**1078–1084.

Ward BA, Gorski JC, Jones DR, Hall SD, Flockhart DA, and Desta Z (2003) The cytochrome P450 2B6 (CYP2B6) is the main catalyst of efavirenz primary and secondary metabolism: implication for HIV/AIDS therapy and utility of efavirenz as a substrate marker of CYP2B6 catalytic activity. *J Pharmacol Exp Ther* **306:**287–300.

Wu S, Moomaw CR, Tomer KB, Falck JR, and Zeldin DC (1996) Molecular cloning and expression of CYP2J2, a human cytochrome P450 arachidonic acid epoxygenase highly expressed in heart. *J Biol Chem* **271:**3460–3468.

Yamaguchi T, Hashizume T, Matsuda M, Sakashita M, Fujii T, Sekine Y, Nakashima M, and Uematsu T (1994) Pharmacokinetics of the H1-receptor antagonist ebastine and its active metabolite carebastine in healthy subjects. *Arzneim-Forsch* **44:**59–64.

Address correspondence to: Dr. Jae-Gook Shin, Dept. of Pharmacology and PharmacoGenomics Research Center, # 633-165, Gaegum-Dong, Busanjin-Gu, Busan 614-735, South Korea. E-mail: phshinjg@inje.ac.kr